Analysis of Three-dimensional Liver Deformation under Free Breathing based on Branching Structure of Potral Vein for MR-guided Focused Ultrasound Surgery

Tatsuhiko Matsumoto[1], Etsuko Kumamoto[1,2], Daisuke Kokuryo[3], and Kagayaki Kuroda[4,5]

[1]*Kobe university, Kobe, Hyogo, Japan,* [2]*Information Science and Technology Center, Kobe, Japan,* [3]*Molecular Imaging Center, National Institute of Radiological Sciences, Chiba, Japan,* [4]*Tokai University, Hiratsuka, Japan,* [5]*Kobe International Frontier Medical Center, Kobe, Japan*

Introduction: In order to apply MRgFUS to the abdominal organs , such as the liver, the target tracking technique is indispensable. Several target tracking methods based on the vessel of the liver has been proposed[1,2]. However, deformation in the liver organs caused by respiratory motion lead to displacement of estimated target position. In this study, we extracted the branched vessels from MRI images by our in-house three-dimensional image processing software, and we analyzed the deformation of the liver organ[3].

Methods and Materials: A series of the multiple sagittal planes in healthy volunteer's liver were acquired by 3.0T MRI (Signa HDxt, GE Healthcare UK Ltd.) with fast image employing steady state acquisition (FIESTA). The imaging conditions were as follows: TR/TE, 4.85/1.98 ms; slice thickness, 5mm; pixel size, 0.68 x 0.68 mm^2; field of view, 350 x 350 mm^2; spatial matrix, 512 x 512; flip angle, 90 degrees. Forty image sets of interleaved six slices were acquired under slow-paced free respiration.

First, we performed thinning of the vessel to the extraction of the branching points: 1) Manually select the center of the blood vessel branching points;, 2) Extract a square (30 × 30 pixels) in each images; 3) Conduct a three-dimensional region to determine the threshold for extracting blood vessel region; 4) Perform smoothing images using a three-dimensional Gaussian filter; 5) Conducted thinning using three-dimensional Euclidean thinning. Next, the coordinates of the branching points were extracted. 3×3×3 filter to extract the coordinates of branch points when three non-adjacent blocks around the filter was applied to extracted thinning vessel images. Displacement of the branch points and distance between several two branched points were arranged for analysis of liver deformation.

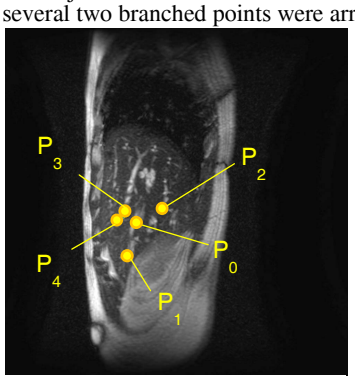

Figure 1 Selected branched points. P_0 was a reference point.

Results: Figure 1 shows branched points for analysis. The distance between the branched point P_0 in the center of the liver and the other branch points (P_1, P_2, P_3, P_4). Distance of P_3 and P_4 are separated about 20 mm to right-left (RL) direction. Figure 2 shows the distance from the reference point P_1 and Figure 2 represents the distance the direction of y-axis. Position of the liver is reduced as the coordinate increases. First, we considered the distance of the branch point at the bottom P_1. These distances extended the position of the liver to become lower. Figure 3 and Table 2 shows that the distance change in the direction of the y-axis (SI) was remarkable. This result shows that liver was compressed by the organs below. On the other hand, the distances between the reference point and the anterior side point P_3, and between the reference point and the posterior side point P_2 were extended. In addition, the posterior side point was extended an even greater distance. This result shows that when the position of the liver falls, the position of the central point also falls. However, the point of the posterior side P_2 was blocked by the spleen. The anterior points were pulled by the posterior point, so the distance was extended between P_0 with P_2. Figure 4 shows that the distance between the other anterior points P_4 had approximately the same y-coordinates as the anterior and posterior points had. The distance to the posterior points extended. This result also proves the previous assumption. Furthermore, P_2 and P_4 extended in RL direction when the position of the liver falls from the results of Figure 4 and Table 2. The software-extracted branching points exhibited that the liver constricts in RL direction for about 12 mm when comes down to inferior with maximum inhalation.

Discussion and Conclusions: Our measurements showed displacement in the liver caused by respiration. The organ largely deforms in z-direction (RL). The amount of constriction when the organ was at the bottom was 12 mm. When extracting the branch point in order to track the tumor, we should choose a branch point that matches the location of the tumor in order to reduce the error caused by deformation. In addition, it is necessary to compare the branch points of locations in the analysis of detailed modifications. Table 1 shows the average errors of the image processing and visually selection. Average error was a maximum of 2.9 mm. On the other hand, the maximum error of the image processing was 8.3 mm. Average error was relatively small. But, it is necessary to consider the support of errors when a sudden displacement occurred.

References [1] Kuroda K, Kokuryo D, et al.: Thermal Medicine; 23(4):181-193, 2007. [2] Kokuryo D, et. al: Proc. of IEEE EMBS 2007; 2614-2617. [3] Kokuryo et al. Magn Reson Med 2012;67(1):156-163.

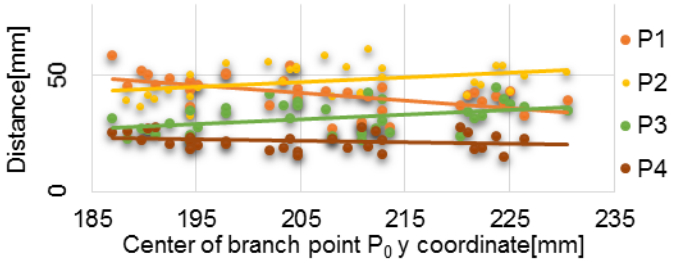

Figure 2 Distance between the branch point P_0 with others. Straight line represents the linear approximation line.

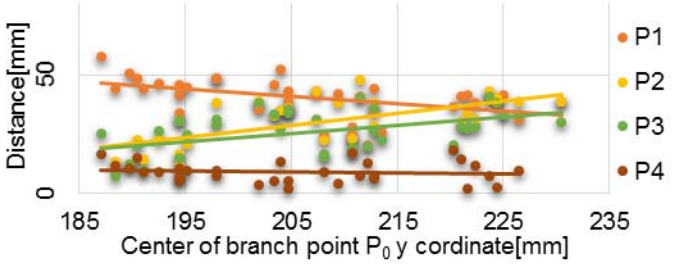

Figure 3 Change of distance in y-axis between the branch point P_0 with others. Straight line represents the linear approximation line.

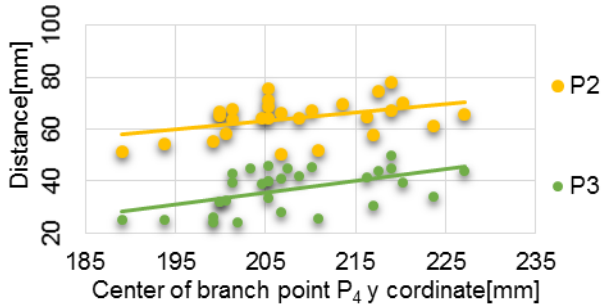

Figure 4 Distance between the anterior side point P_4 with P_2 and P_3.

Table 1 The average errors of the image processing and visually selected. These numerical value is distance between P_0 with others [mm].

	P_1	P_2	P_3	P_4
Average error [mm]	2.90	1.92	2.75	2.05
Maximum error [mm]	8.26	7.90	6.71	7.86

Table 2 The gradients of the fitted curve in x and z axis between the branch point P_0 with others. Position of the liver is reduced as the coordinate increases.

	P_1	P_2	P_3	P_4
x-axis gradients	-0.10	-0.08	-0.05	-0.09
z-axis gradients	-0.14	-0.25	-0.10	0.07